Jasmonic acid and salicylic acid interact to determine spatial regulation of gene expression response in leaf to herbivore and mechanical wounding

Valentina Levak[1,2,*], Tjaša Mahkovec Povalej[1], Karmen Pogačar[1,2], Katja Stare[1], Maja Zagorščak[1], Tim Hawkins[3], Joanne Robson[3], David Dobnik[1], Tjaša Lukan[1,†], Kristina Gruden[1,*,†]

1 Department of Biotechnology and Systems Biology, National Institute of Slovenia, Ljubljana, Slovenia

2 Jožef Stefan International Postgraduate School, Ljubljana, Slovenia

3 Department of Biosciences, Durham University, Durham, UK

† shared last authorship

* corresponding authors

Supplementary Figures

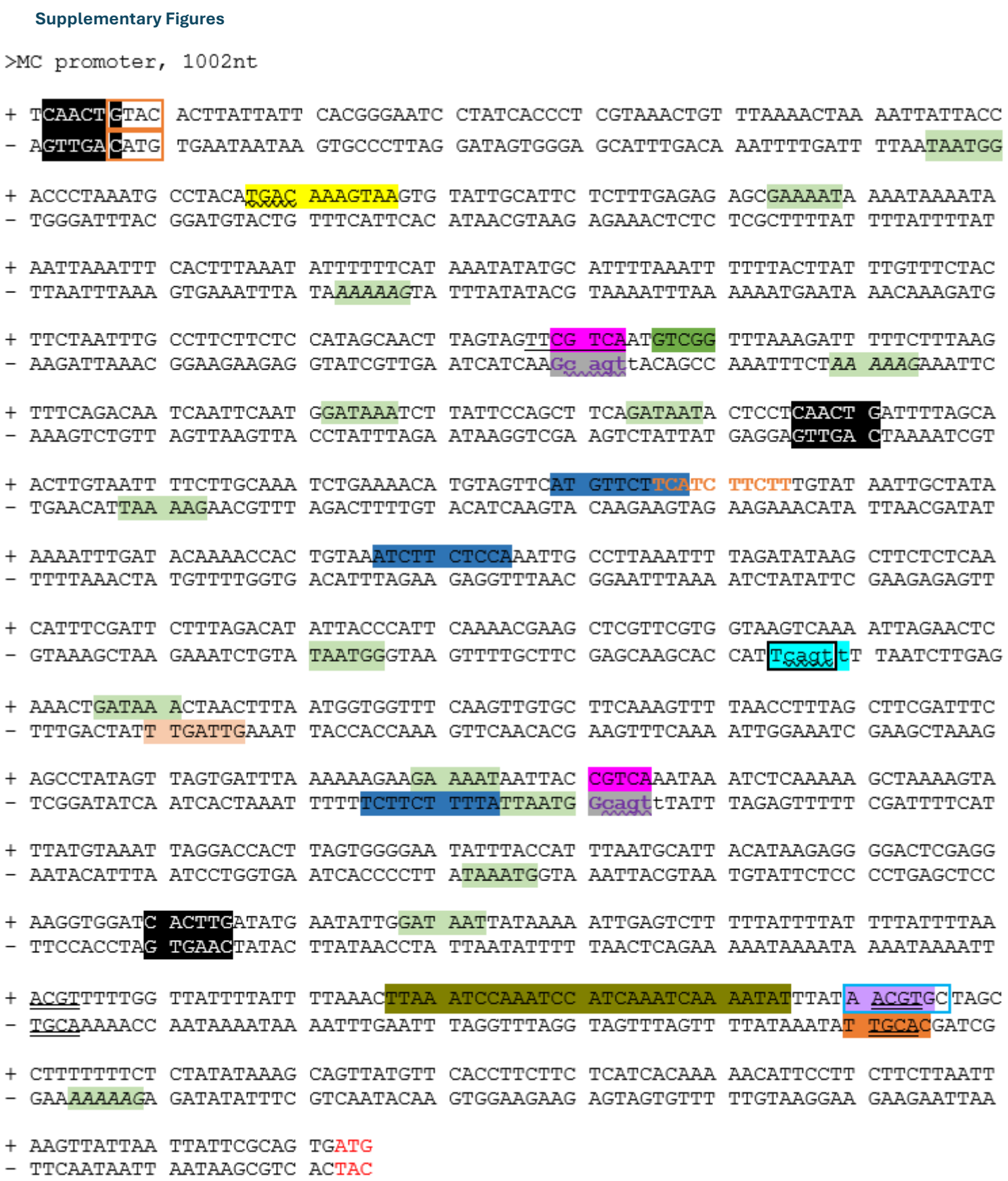

Figure S1: *MC* promoter is predicted to contain many defense-response-related cis-regulatory elements. Visual representation of predicted regulatory elements of *MC* promoter (1002 bp) from S. tuberosum cv. Desiree that was used in sensor potato plants. The predicted regulatory elements involved in biotic stress responses are CGTCA-motif (involved in the MeJA-responsiveness; pink), TC-rich repeats (involved in defense and stress responsiveness; blue), TGACG-motif (involved in the MeJA-responsiveness; grey), G-box (involved in defense responsiveness; dark orange),

TGA1A binding site (TGA1a transcription factor recognition site, underlined), WRKY (WRKY binding site; yellow), DREB1B (involved in tobacco streak virus infection and PR gene expression; dark green), AT4G12670 (involved in SA and JA responsiveness; dark yellow), MYCCONSENSUAT (MYC recognition site; white on black), GT1CONSENSUS (consensus GT-1 binding site, influences the level of SA-inducible gene expression; light green), WRKY71OS (a core of TGAC-containing W-box WRKY binding site within the Pathogenesis-Related Class10 (PR-10) genes; zig zag underlined), WBOXATNPR1 (W-box, recognized by salicylic acid (SA)-induced WRKY DNA binding proteins; lowercase), ACGTATERD1 (involved in Ca2+ responsiveness; double underlined), ASF1MOTIFCAMV (ASF-1 binding site, involved in salicylic acid and biotic stress responsiveness; purple bold letters), GT1GMSCAM4 (involved in pathogen responsiveness; italic), CURECORECR (involved in oxygen response; bordered with orange), TCA1MOTIF (involved in SA responsiveness; orange bold letters), T/GBOXATPIN2 (involved in JA responsiveness; purple), MYB1LEPR (G-box, Tomato Pti4(ERF) regulates defense-related gene expression via GCC box; light orange), ABRERATCAL (involved in Ca2+ responsiveness; bordered with light blue), WBOXNTERF3/WBOXHVISO1 (W-box; bordered with black), WBBOXPCWRKY1 (WB/W box, WRKY proteins binding site in PR1 gene in parsley; bordered with turquoise). The ATG (red letters) indicates the start of MC coding region. The promoter region is located upstream of the ATG. The predictions were obtained with PlantCARE, Transfac and PLACE. The complete list of MC promoter domains from potato cv. Désirée with their positions and sequence, predicted with PlantCARE, Transfac, and PLACE are specified in Table S1.

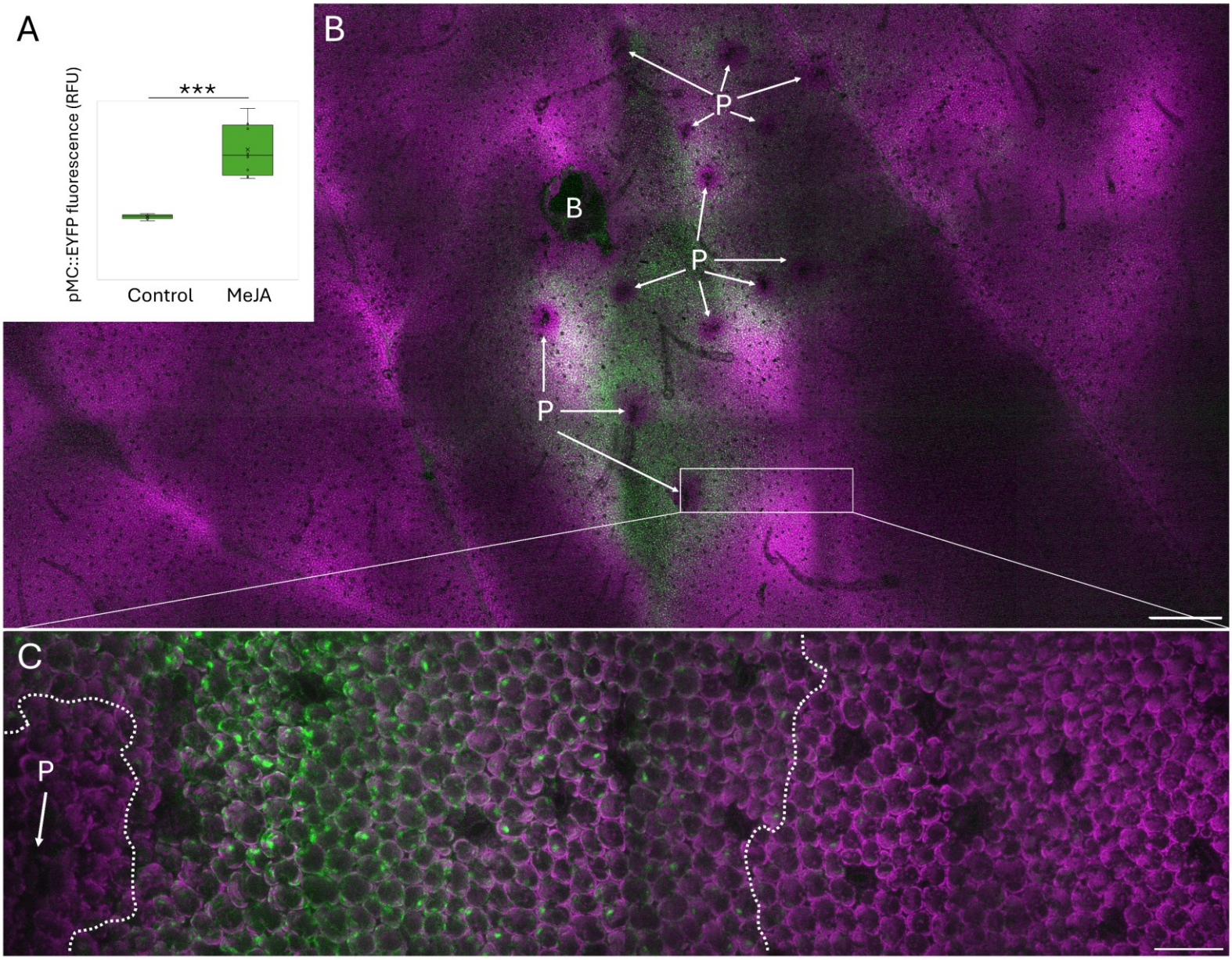

Figure S2: Responsiveness of p*MC::EYFP* sensor in an independent transgenic line (line 18) to CPB feeding. (A) Barplot showing the induction by MeJA treatment. Fluorescence intensity was quantified in images of samples from 2-3 leaves of 3 plants per group as mean fluorescence. Statistical differences were calculated with Student's t-test. ***: $p < 0.001$. (B) Overview of CPB larva woundings on the potato leaf. BW: bite wound, P: probing wounds are pointed. Overlay of chlorophyll (purple) and EYFP (green) channels are shown. Scale bar, 1 mm. (C) Closeup image that shows response to one of the probing wounds (pointed with arrow). The border of the observable response is shown with dotted line. Scale bar, 100 µm. Responsiveness to same conditions of another *pMC::EYFP* independent transgenic line (line 14) is shown on Figure 1C–E in the main text. Raw images can be found at Zenodo: 10.5281/zenodo.16875336

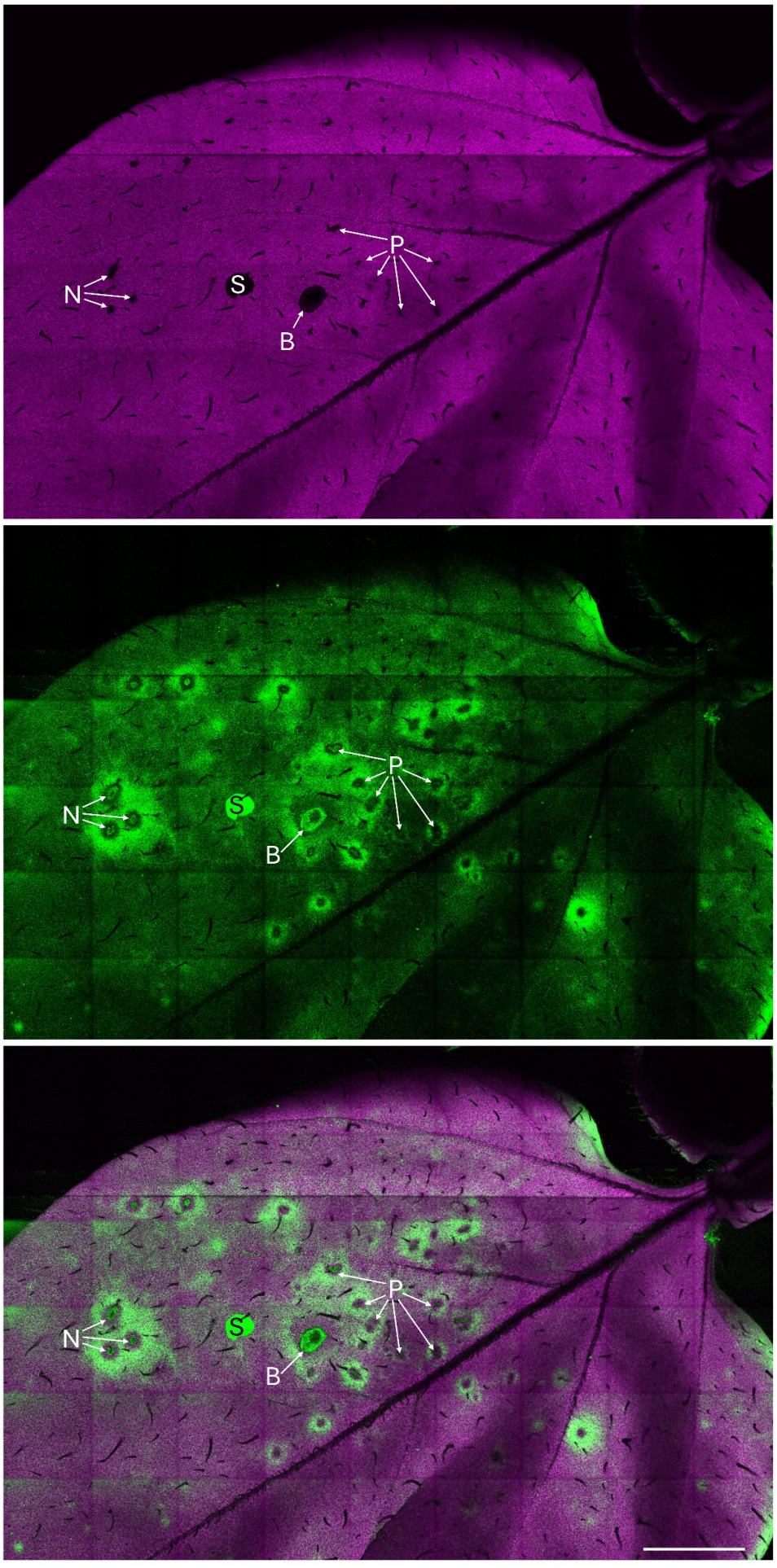

Figure S3: Result of another independent experiment of p*MC::EYFP* response 20 h after wounding treatments. Top: chlorophyll autofluorescence, middle: EYFP fluorescence, bottom: overlay of both channels. BW: bite wound, P: probing wounds, NW: needle wounds, S: saliva autofluorescence in EYFP channel. Scale bar, 5 mm. Raw images can be found at Zenodo: 10.5281/zenodo.16875336

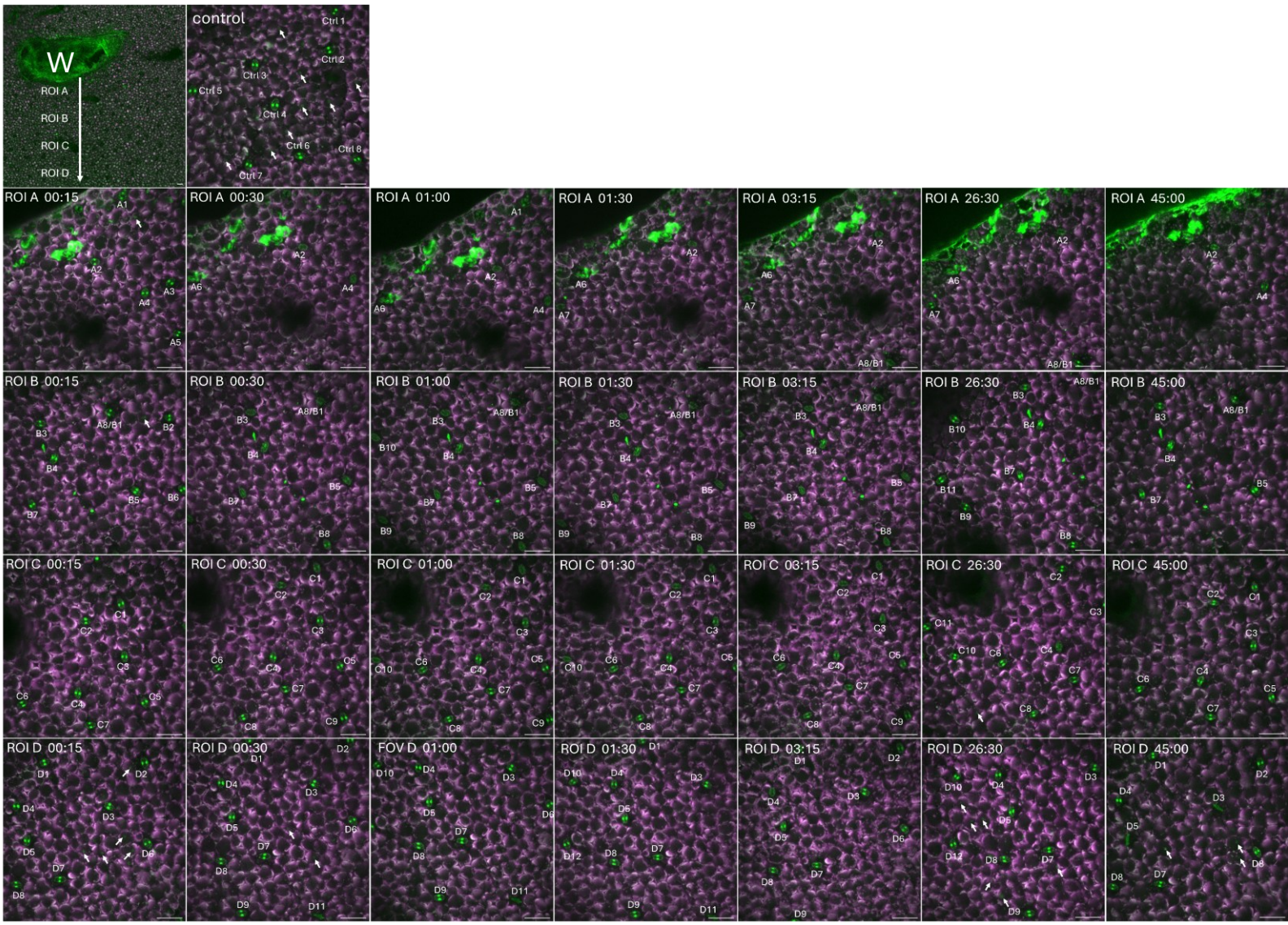

Figure S4: Jas9-Venus-N7 response before (control) and at different times after CPB bite wounding. Scale bar, 100 µm. Results for potato cv. Rywal, transgenic line 1 are shown. Stomata in which Jas9-Venus-N7 signal was quantified (Table S2, CPB) are indexed. Results of quantification are presented in the main text, Figure 3A. Some palisade tissue nuclei with Jas9-Venus-N7 are pointed with arrows. W: CPB bite wound. Image in higher resolution and raw images can be found at Zenodo: 10.5281/zenodo.16875336

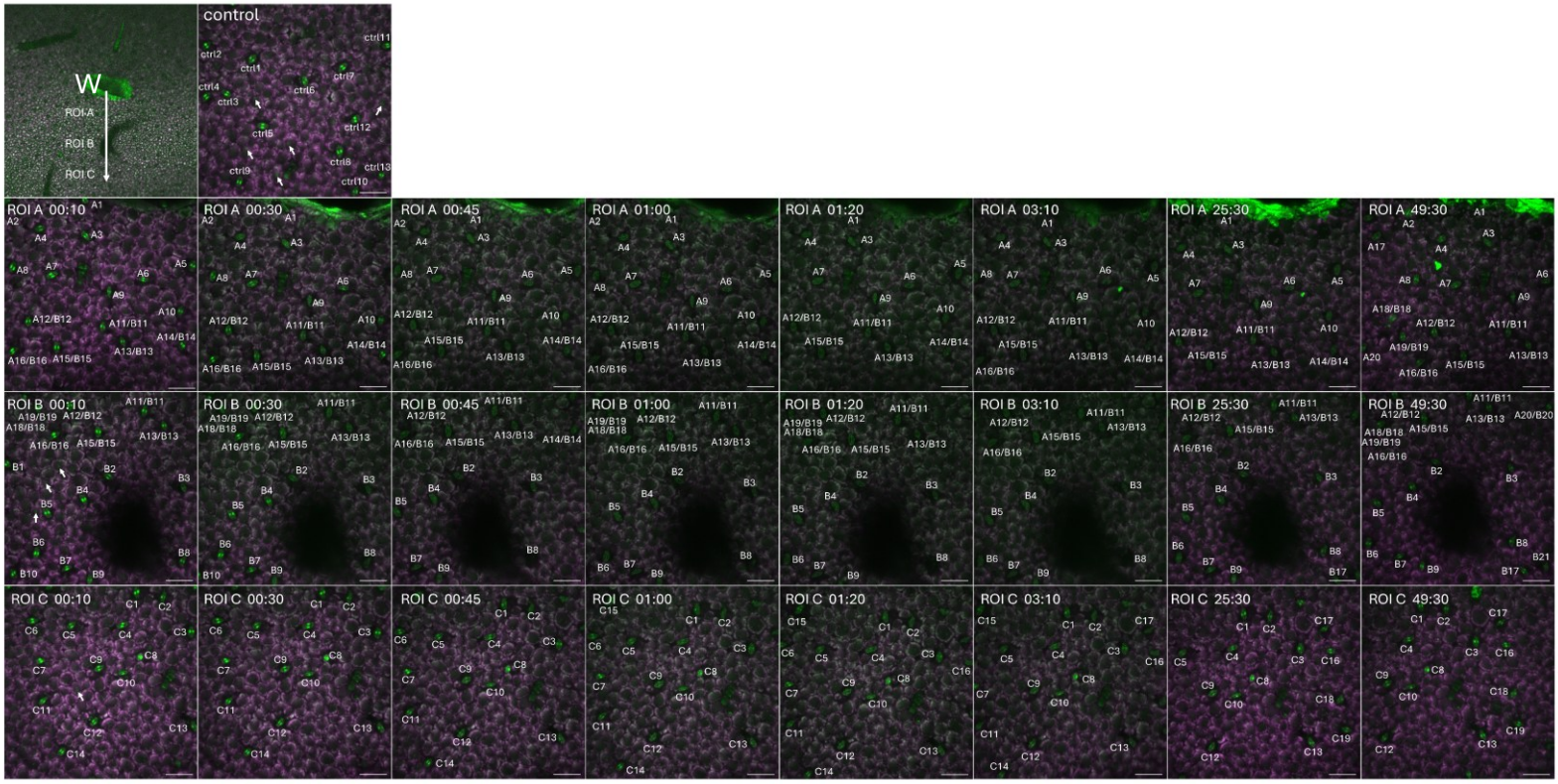

Figure S5: Jas9-Venus-N7 response before (control) and at different times after needle wounding. Results for potato cv. Rywal, transgenic line 1 are shown. Overlays of Venus (green) and chlorophyll (purple) channel are shown. Scale bar, 100 µm. Stomata in which Jas9-Venus-N7 signal was quantified (Table S2, NW) are indexed. Some palisade tissue nuclei with Jas9-Venus-N7 are pointed with arrows. W: needle wound. Image in higher resolution and raw images can be found at Zenodo: 10.5281/zenodo.16875336

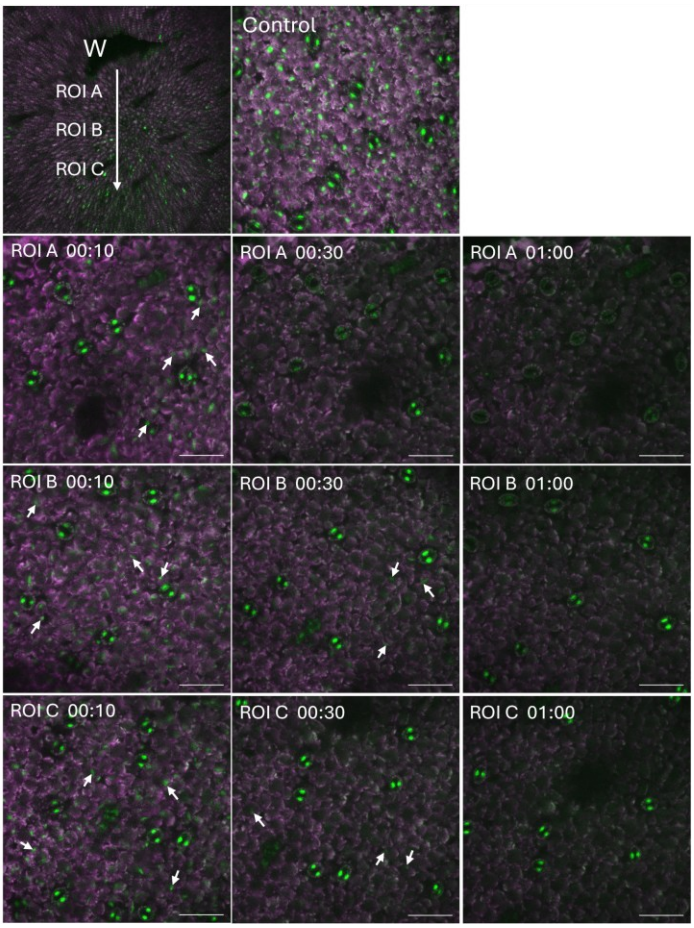

Figure S6: Jas9-Venus-N7 response before (control) and at different times after needle wounding in another independent transgenic line. Jas9-Venus-N7 signal was measured in an independent transgenic line of potato cv. Désirée, transgenic line 6, in tissue culture. Overlays of Venus (green) and chlorophyll (purple) channel are shown. Scale bar, 100 µm. Some epidermal and palisade tissue nuclei with Jas9-Venus-N7 are pointed with arrows. W: needle wound. Mind the signal in the stomata, epidermal and palisade tissue is decreasing with time at increasing distance from the wound. Image in higher resolution and raw images can be found at Zenodo: 10.5281/zenodo.16875336

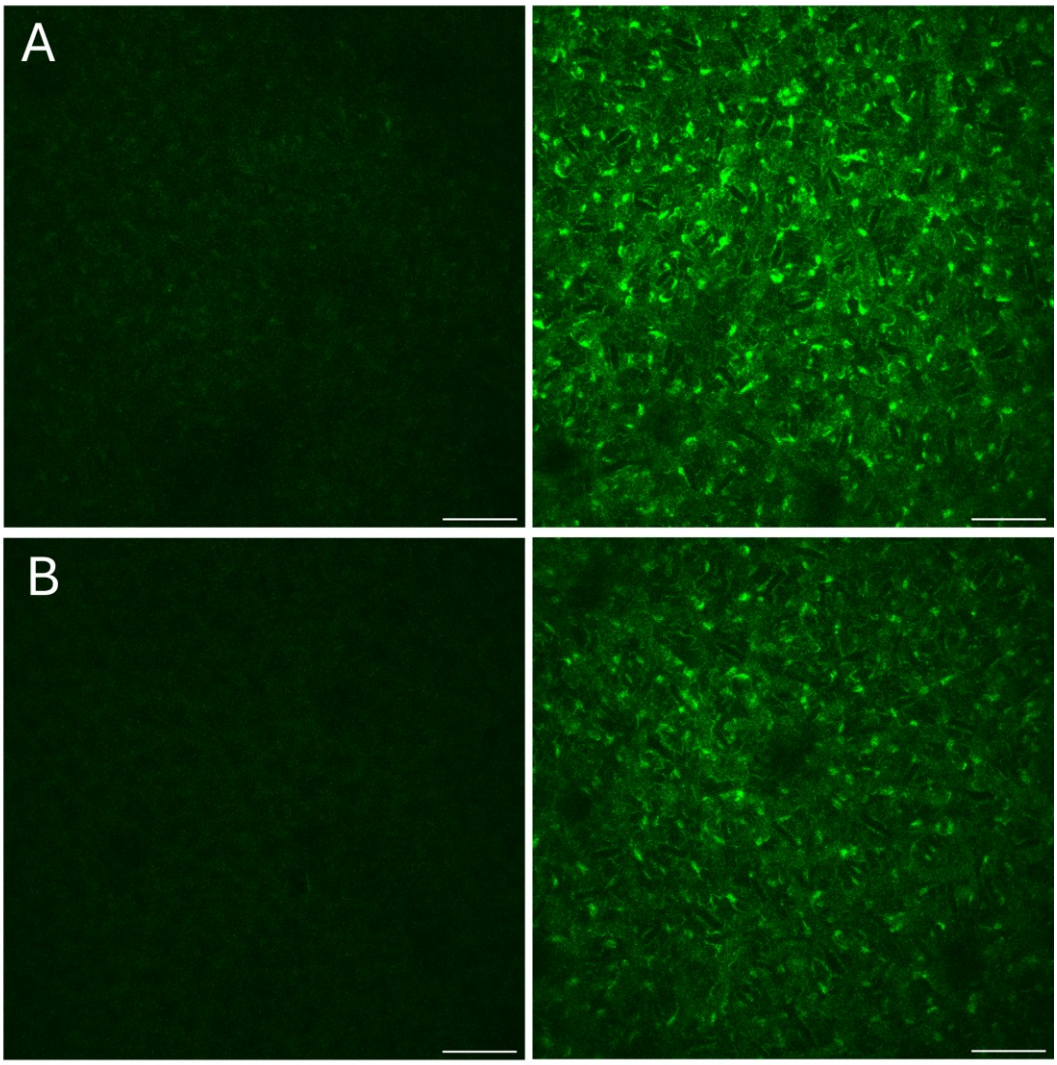

Figure S7: *pMC::EYFP* transgenic lines in *NahG* background are inducible to MeJA. *pMC::EYFP* response in *NahG* background in two independent transgenic lines. Line 7 (A) and line 12 (B) treatment were confirmed for their inducibility to MeJA after 24 h. Left: mock, right: MeJA. EYFP channel is shown. Scale bar, 100 µm. Raw images of these two and two more independent transgenic lines can be found at Zenodo: 10.5281/zenodo.16875336

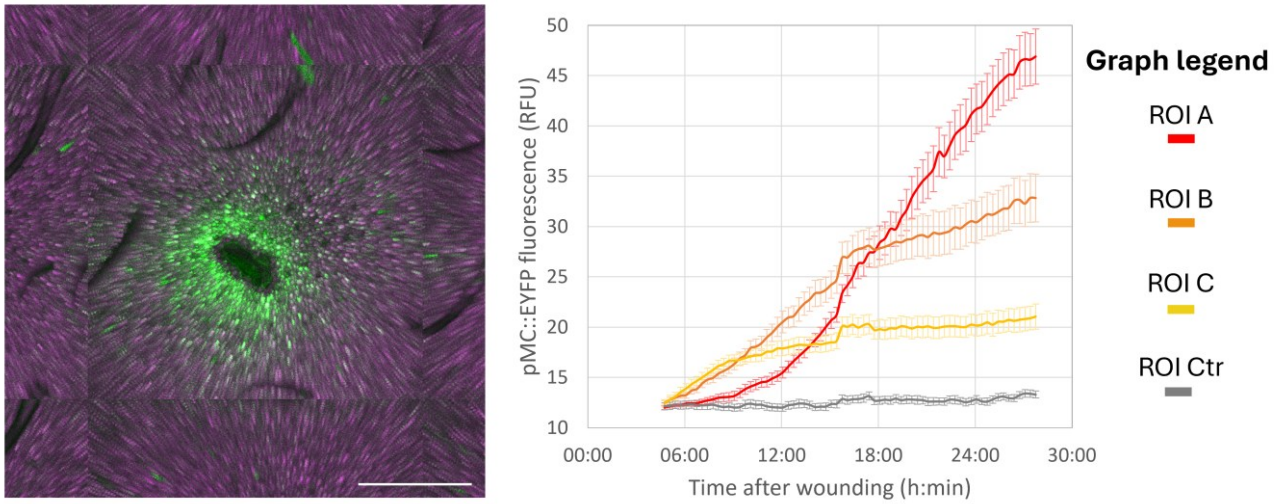

Figure S8: *pMC::EYFP* response to mechanical wounding in an additional transgenic line with *NahG* background. *pMC::EYFP* response in an additional independent transgenic line (line 7) with *NahG* (SA-depleted) background. Left image shows *pMC::EYFP* response 24 h after wounding with a needle (overlay of chlorophyll channel in purple and EYFP channel in green) and graph on the right shows temporal response in ROIs: ROI A (cells closest to the wound, marked as in nontransgenic background) in red, ROI B (cells next to ROI A) in orange, ROI C (cells outwards ROI B) in yellow, ROI Ctr (cells further away without increase of *pMC::EYFP* signal in grey). Scale bar, 1 mm. Average response in the distinctive ROIs with standard error is shown in graphs on the right. Responsiveness to same conditions of another *pMC::EYFP* independent transgenic line (line 12) is shown on Figure 3E in the main text. Movie of the timeseries of can be found in Supplement (Movie S4) and at Zenodo, together with raw images: 10.5281/zenodo.16875336. The latter includes also raw images of timeseries following wounding of two more independent transgenic lines *pMC::EYFP* in *NahG* background.

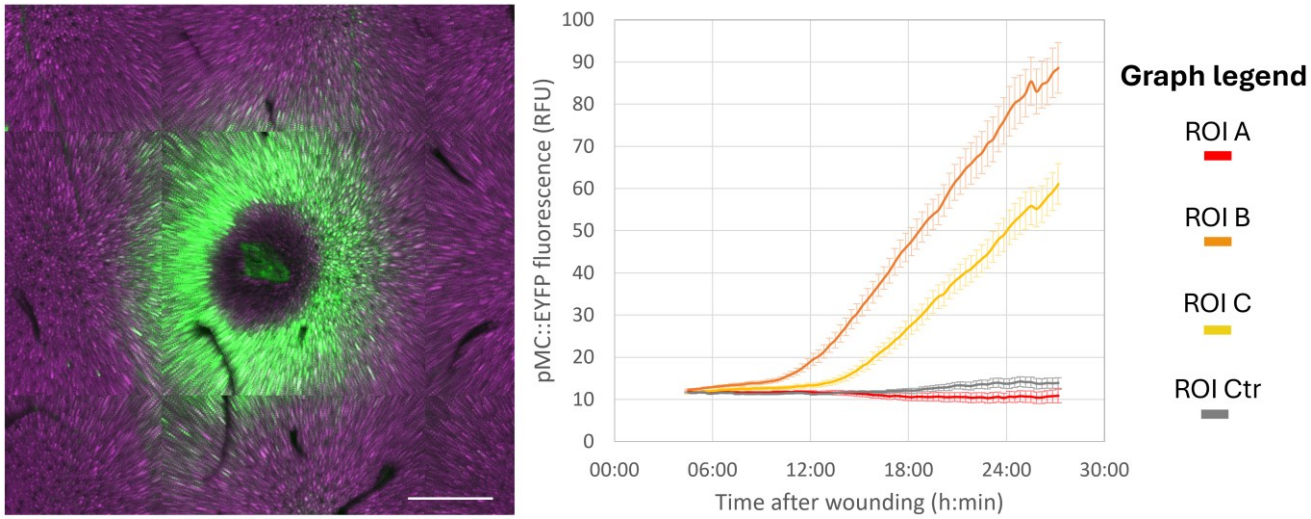

Figure S9: *pMC::EYFP* response to mechanical wounding in nontransgenic background. Left image shows *pMC::EYFP* response 24 h after wounding with a needle (overlay of chlorophyll channel in purple and EYFP channel in green) and graph on the right shows temporal response in ROIs: ROI A (cells closest to the wound, marked as in nontransgenic background) in red, ROI B (cells next to ROI A) in orange, ROI C (cells outwards ROI B) in yellow, ROI Ctr (cells further away without increase of *pMC::EYFP* signal in grey). *pMC::EYFP* response in this nontransgenic background (line 18) can be compared with *pMC::EYFP* response in *NahG* background (shown on Figures 3E in the main text and S8 in the Supplementary Figures) – mind the different response in ROI A between both background genotypes. Scale bar, 1 mm. Average response in the distinctive ROIs with standard error is shown in graphs on the right. Movie of the timeseries can be found in Supplement (Movie S6) and at Zenodo, together with raw images: 10.5281/zenodo.16875336

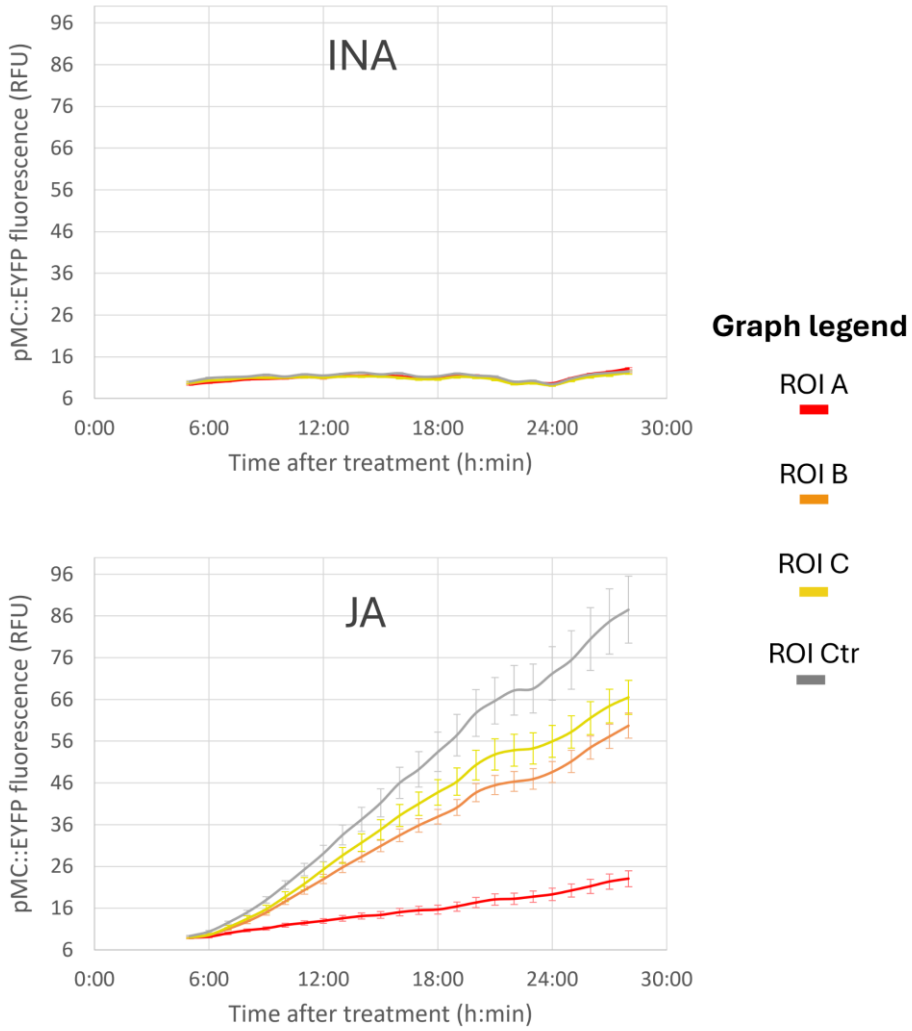

Figure S10: Response to wounding following INA and JA treatment in another independent transgenic line (line 14). *pMC::EYFP* response in nontransgenic background after treatment with SA analogue INA (2,6-dichloronicotinic acid) or JA followed by mechanical wounding (piercing the leaf with a sterile needle). Graphs show temporal response in ROIs: ROI A (cells closest to the wound) in red, ROI B (cells next to ROI A) in orange, ROI C (cells outwards ROI B) in yellow, ROI Ctr (cells further away). Average response in the distinctive ROIs with standard error is shown. Responsiveness to same conditions of another *pMC::EYFP* independent transgenic line (line 18) is shown on Figure 3F in the main text. Movies of the timeseries can be found in Supplement (Movies S11 and S12) and at Zenodo, together with raw images: 10.5281/zenodo.16875336

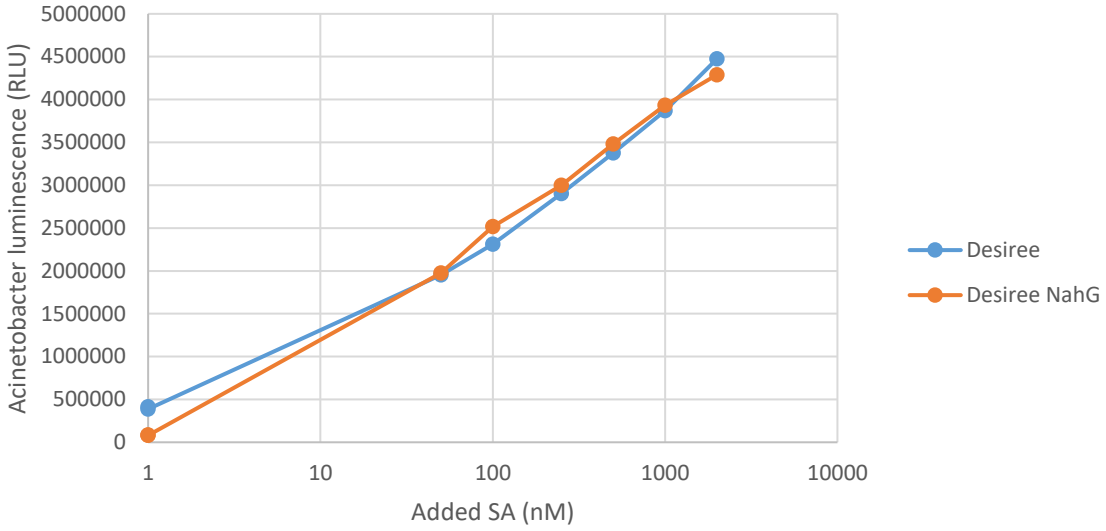

Figure S11: Standard curve of Acinetobacter ADPWH_*lux* measurement of salicylic acid (SA). Leaf homogenates from potato cv. Désirée and Désirée–NahG were spiked with increasing final SA concentrations and assayed with Acinetobacter ADPWH_*lux*. Resulting luminescence values were used to generate calibration curves; the cv. Désirée curve served to calculate SA increases reported in Figure 3D.